Journal of Ceramic Processing Research. Vol. 12, No. 4, pp. 456~461 (2011)

JOURNAL OF
Ceramic
Processing Research

Easy synthesis of highly monodispersed silica@M (M = Ag, Au, Pd, Pt) particles using thiol compounds as a connecting agent

Jae-Hyung Park[a], Yong-Geun Lee[b] and Seong-Geun Oh[b,*]

[a]*R&D Management Team, Korea Institute of Energy Technology Evaluation and Planning(KETEP), Teheran-ro 114gil 14, Gangnam-gu, Seoul, 135-502, Republic of Korea*

[b]*Department of Chemical Engineering, Hanyang University, 17 Haengdang-dong, Seongdong-gu, Seoul 133-791, Republic of Korea*

Silica@M (M = Ag, Au, Pd, Pt) particles were prepared by accumulating noble metal nanoparticles on the surface of thiol-functionalized silica as a substrate, which was accomplished by the strong interaction between noble metal nanoparticles and thiol groups. In the conventional method, the fabrication of metal coated silica spheres by LBL (layer-by-layer) or core-shell synthesis is not efficient due to the complexity of the synthetic method, the low surface coverage of functional groups on the particles, and the low loading capacity of noble metal particles. The synthetic method in this study could overcome these limitations and make possible the simple preparation of the silica@M (M = Ag, Au, Pd, Pt) and hollow Pt metal particles with substantial metallic layers via a self-assembly behavior by a strong interaction between noble metal nanoparticles and thiol groups. Detailed characterizations of the silica@M (M = Ag, Au, Pd, Pt) and hollow Pt metal particles were performed to elucidate the surface and structural properties, the coordination of noble metals, and the crystalline structure of the noble metals on the surface by various analytical methods.

Key words: Silica@noble metal particles, Sol-gel reaction, Silica, Coating, Hybrid particles.

Introduction

In recent years, the investigation of unique hybrid materials is attractive in the fields of chemistry and physics. For instance, many research groups have devoted attention to the preparation of metal coated composite particles due to their potential application in various fields of catalysis, surface-enhanced Raman scattering (SERS), photonics, information storage, and biochemistry for sensors and antibacterial materials [1-7]. In particular, colloidal silica is a useful material as a substrate for a hybrid material in colloidal science. Since Stöber *et al.* first reported the synthesis of silica spheres in 1968 [8], the well-known Stöber-Fink-Bohn (SFB) process has been investigated and discussed to control the size distribution and shape depending on the various synthetic factors such as temperature, pH, and concentration of reactants [9-10] because these silica spheres being efficient candidates for applications including optical devices, separations and adsorbents.

One of the most important approaches to fabricate metal coated silica composite particles (silica@metal particles) is the surface modification of silica particles by introducing the organic chemicals. By using an organosilane, the organic source including a thiol [12-14], amine [14-16], vinyl [17], or other organic groups [18] can be immobilized to the surfaces of silica spheres. Surface modification offers the possibility for successive deposition of diverse materials. However, the main disadvantage of the traditional strategy is the relatively low grafting density of organic groups. When bare silica particles are used as substrates, many organic groups cannot be attached at the silica surfaces [19] because silica spheres prepared through the SFB process have a nonporous property. In addition, inconvenient multi-step processes are usually needed for the preparation of the substrate material. In the formation of composite particles, metal nanoparticles were immobilized onto various inorganic supports through alternative routes which were used to control the morphology with the property of nano-materials [20-22]. In order to synthesize metal-silica hybrid particles, the surface modified silica particles have to be redispersed in a reaction medium, and then metal ions are reduced to the metal nanoparticles. However, such proceeding steps are not only complicated, but also expensive for practical applications [23, 24]. Furthermore, the deposition intensity of metal nanoparticles onto the silica surfaces is low due to the limited coverage of surface modifying groups. Therefore, there is a need for suitable substrates onto which can be loaded many metal nano-particles and such research is still a challenge to find a proper process to synthesize these composite materials.

In this study, we describe a simple, reproducible, and scalable method to prepare monodispersed metal-silica composite particles. The synthesis of monodispersed silica particles as a substrate is achieved via our previous study

*Corresponding author:
Tel : +82-2-2220-0485
Fax: +82-2-2294-4568
E-mail: seongoh@hanyang.ac.kr

[25]. Because the silica substrates having many thiol groups on their surfaces were made using only organosilane (MPTMS) without any other precursors, for example tetraethyl orthosilicate (TEOS) or tetramethyl orthosilicate (TMOS), many metal nanoparticles can be attached easily on the silica substrates. This approach has been tested with various noble metal ions such as Ag, Au, Pt, and Pd. Moreover, these composite materials prevent agglomeration of metal nanoparticles without the use of a stabilizer and are easily retrieved due to the relatively large size of the silica substrates. Besides, we can prepare the hollow Pt particles through the removal of the silica template with HF. To the best of our knowledge, this is the first report about synthesizing with such a selective etching strategy.

Materials and Methods

Materials

The 3-mercaptopropyltrimethoxysilane (MPTMS) and sodium borohydride ($NaBH_4$, 99%) as a reducing agent were purchased from the Sigma-Aldrich chemical company, and ammonium hydroxide (NH_4OH 25%, Wako Pure Chemical Industries, Japan) was used as a catalyst. Silver nitrate ($AgNO_3$ 99.995%, Aldrich) as a silver ion source, palladium (II) nitrate dihydrate ($Pd(NO_3)_2 \cdot nH_2O$, n = 2, Aldrich) as a palladium ion source, hydrogen tetrachloroaurate (III) hydrate ($HAuCl_4 \cdot nH_2O$, n = 3.7, Kojima Chemicals) as an Au ion source, hexachloroplatinate (IV) hydrate ($H_2PtCl_6 \cdot xH_2O$, x = 5.6, Kojima Chemicals) was used as a platinum ion source. All chemicals were used as received without further purification. Water was obtained from a Milli-Q water purification system (Millipore).

Preparation Method

Preparation of thiol-functionalized silica (MPTMS silica) particles

The 10 g of MPTMS was added into 100 g of water with stirring until the oil (MPTMS) droplets had completely disappeared and a transparent solution was obtained. NH_4OH (0.1 ml) was added to the mixture solution, and then the solution was kept at room temperature for 12 h.

Preparation of noble metal coated MPTMS silica particles and Pt hollow spheres

To prepare the silica@M (M = Ag, Au, Pd and Pt) particles, thiol functionalized silica particles (1 g) were dispersed in 150 ml of an aqueous solution with 30 minutes ultrasonication. The solution was cooled to 4 °C, and then 0.1 g of metal source and 3 ml of NH_4OH were added into the solution with stirring vigorously. After about 10 minutes, 10 ml of ice-cold 0.132 g $NaBH_4$ solution was added to the solution at 4 to 80 °C. By increasing the temperature from 4 to 80 °C, the formation, attachment and accumulation of the noble metal nanoparticles on the MPTMS silica particles were induced for 10 h. As the reaction proceeded, the color of the solution was changed to a rich color. The final step involved the removal of the silica template by treating the silica@Pt particles with 5 M HF to produce hollow Pt spheres.

Characterization

Field emission scanning electron microscopy (FE-SEM, JEOL Co. Models JSA 840A and JSM-6700) was used to investigate the morphology of the silica@M (M = Ag, Au, Pd and Pt) particles. The transmission electron microscopy (TEM) pictures were taken through a JEOL JEM-2000EXII microscope working at 200 kV. The samples for TEM were obtained by dispersing small drops of the suspension with a much lower concentration onto copper grids pre-coated with amorphous carbon. X-ray photoelectron spectroscopy (XPS) measurements were performed with an electron spectroscopy for chemical analysis system (ESCA, Omicron EA125, Philadelphia, PA) using a Mg K source at 1253.6 eV. The X-ray power supply was operated at 200 W (20 mA × 10 kV). The pressure in the analysis chamber during scans was kept below 2×10^{-10} mm Hg (2.67×10^{-8} Pa).

Results and Discussion

The simple strategy to fabricate noble metal coated silica particles [silica@M (M = Ag, Au, Pd, Pt) particles] without the additional surface modification process is shown in Fig. 1. First, the MPTMS silica spheres which were synthesized by the one-step method as in our previous study and the metal ions were distributed homogeneously in the aqeous solution, and some metal ions would be adsorbed through electrostatic attraction on the surface of the MPTMS silica spheres. Second, the reduction process would be initiated on the surface of MPTMS

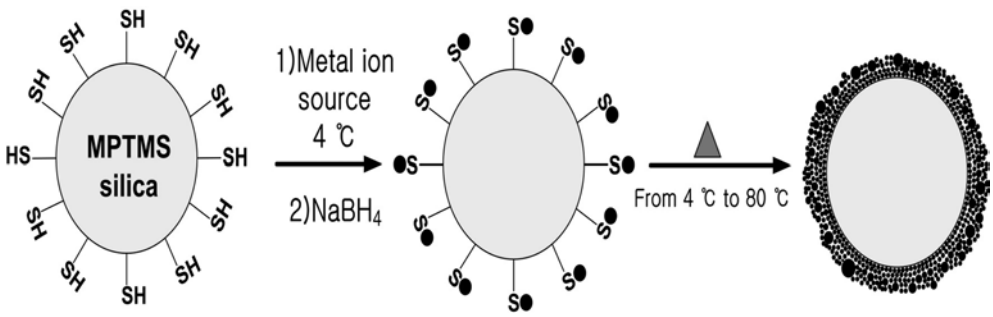

Fig. 1. Schematic illustrations of major steps involved in the synthesis of MPTMS silica@M (M = Ag, Au, Pd and Pt) particles.

silica spheres by adding sodium borohydyride ($NaBH_4$). The initially created metal nanoparticles are combined with the terminal thiol groups of MPTMS silica spheres via chemisorption. Because the pH is maintained at about 12, desorption of metal nanoparticles does not occur in this system [13, 14]. Thus, during the reduction process at 4 °C, this leads to the formation and immobilization of the metal nanoparticles on the silica surfaces. This is followed by the reduction of nanoparticles that were generated at a low temperature (at 4 °C for 2 h) onto MPTMS silica spheres via chemisorption with the thiol groups. A further explanation for the chemical mechanism, the thiol groups attach to the metal ions by the cleavage of S-H bonds and the spontaneous formation of S-metal bonds [26]. As a result of the unique behavior of thiol groups containing a sulfur atom, chemicals containing thiol groups have been widely used as chemical protocols to make various metal-polymer and metal-metal oxide composites. Third, increasing the temperature from 4 to 80 °C for 10 h eventually led to the formation of metal-coated silica spheres surrounded by numerous metal nanoparticles (the growth process). This strategy led to the surfaces of MPTMS silica spheres being covered by metal nanoparticles as seeds, which provide the nucleation sites for the new growth of metal overlayers. However, the size of the metal nanoparticles at the outer wall in the silica spheres was larger than that of the metal nanoparticles size at the inner wall in the silica spheres. The size of metal nanoparticles tends to increase at high temperature [13].

To determine whether a thiol group has been formed in the one-step synthetic method and to get information on the basic molecular structure of the as-synthesized MPTMS silica spheres, FT-IR measurements were performed. Fig. 2 shows FT-IR spectra of MPTMS silica spheres by the one-step method in our previous study and MPTMS silica after calcination at 500 °C for 5 h. The asymmetric stretching vibrations of the siloxane (Si-O-Si) appear between 1000 and 1200 cm^{-1}, and the symmetric stretching vibrations of the siloxane (Si-O-Si) appear at 800 cm^{-1} in the spectra of all the samples [27-30]. The band at 3700-3200 cm^{-1} which is attributed to the stretching vibration of Si-OH in the silanol group is also a typical band of silica, and the broad peaks at ~3350 and 1620 cm^{-1} indicated that silica contains large amounts of adsorbed water from atmospheric moisture [27]. In case of MPTMS silica (Fig. 2(A)), we could detect all the typical band of silica and the weak stretching vibration of the thiol groups (S-H) are revealed at 2560 cm^{-1} [27, 30, 31]. Additionally, the bands at 2924 and 2858 cm^{-1} are the asymmetric and symmetric stretchings of methylene groups (CH_2) in the mercaptan moiety of MPTMS [27, 28]. However, there were no bands at 2560 cm^{-1} of the thiol groups (S-H), and around 2924 cm^{-1} of the methylene groups (CH_2) in FT-IR spectrum for MPTMS-C which was measured after calcination at 500 °C for 5 h (Fig. 2(B)) because most surface and internal thiol and methylene groups are eliminated by the calcination process [30]. Furthermore, the FT-IR spectrum of MPTMS silica spheres indicated doublet peaks in 1200-1000 cm^{-1} of the asymmetric stretching vibrations of the siloxane (Si-O-Si). This result reveals that the Si-O-C bond is certainly obtained by condensation of MPTMS [32].

Fig. 3 shows SEM images of silica@M (M = Ag, Au, Pd and Pt) particels prepared by the typical reaction

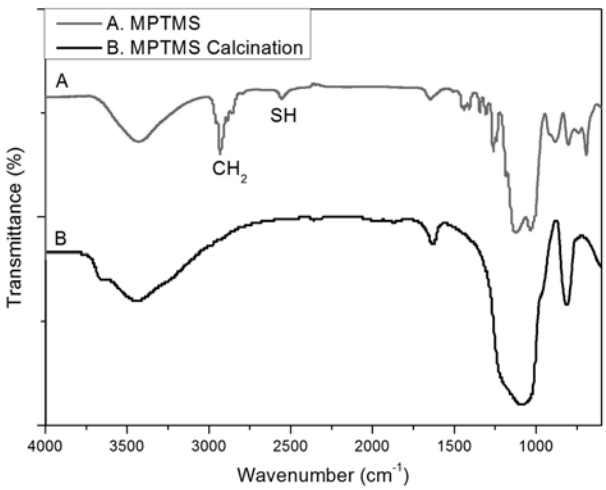

Fig. 2. FT-IR spectra of (A) as-synthesized MPTMS silica, (B) MPTMS silica after calciantion at 500 °C for 5 h.

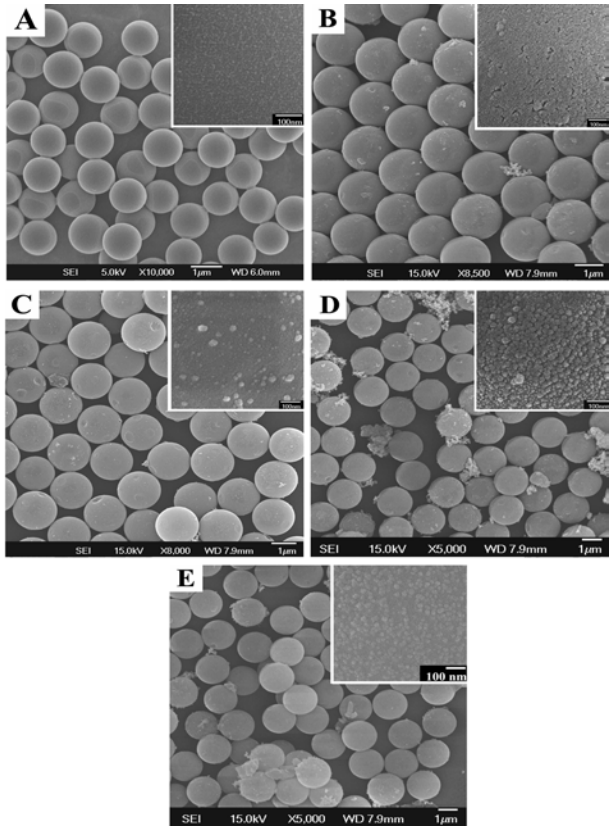

Fig. 3. SEM images of (A) Bare MPTMS silica, (B) MPTMS silica@Ag, (C) MPTMS silica@Au, (D) MPTMS silica@Pd, and (E) MPTMS silica@Pt (insets are magnified images of the surface morphologies).

conditions. Bare silica (Fig. 3(A)) made of MPTMS presents uniform monodisperse spherical particles with an average diameter of about 1.6 μm and smooth external surface (inset of Fig. 3(A)). It is possible to synthesize highly monodipersed MPTMS silica particles by the unique self-hydrolysis phenomenon of MPTMS which is easily hydrolyzed into organosilanetriol by self-hydrolysis in the aqueous solution contrary to the case of insoluble TEOS. On the other hand, the surface morphologies of silica@M (M = Ag, Au, Pd and Pt) particles (inset of Fig. 3(B), (C), (D), (E)) show obviously rough surfaces, and some aggregated metal particles were revealed in each sample (Fig. 3(B), (C), (D), (E)) compared with the those of bare silica.

To further determine whether noble metals have been coated on the surface of MPTMS silica sheres and to get information on the intensity of crystallization, XRD measurements were performed. The XRD patterns of silica@M (M = Ag, Au, Pd and Pt) particles are shown in Fig. 4. The Bragg peaks in the 2θ range of 35-80° can be attributed to the face-centered-cubic (fcc) structure of Ag (Fig. 4(A) curve) and Pd (Fig. 4(C)) as (111), (200), (220) and (311) reflections, which are all good accordance with the diffraction data from the JCPDS cards. Also, the diffraction peaks of Fig. 4(B) and (D) confirm the Au and Pt fcc structure indicated by (111), (200) and (220) reflections. Furthermore, the intensity of XRD peaks is closely related not only to the degree of crystallinity but also to the quantity of crystals existing in the sample. Although Fig. 4(C) of silica@Pd shows a stronger intensity of the main peak than the other samples, this result does not indicate that silica@Pd has a large thickness of the coated palladium layer because Fig. 3(D) shows that Pd nanoparticles and silica@Pd coexisted in the sample. In the case of silica@Pt, however, Fig. 4(D) shows a relatively strong intensity of the main peak although Pt nanoparticles are rarely found in the sample (Fig. 3(E)). This means that silica@Pt has a large relative thickness of the coated platinum layer. Therefore, we can interpret that the real thickness of the coated palladium layer in silica@Pd is relatively thin, and the XRD pattern shows that the variations in signal intensity are predominantly due to the difference in the interaction strength between noble metal nanoparticles and thiol groups [14].

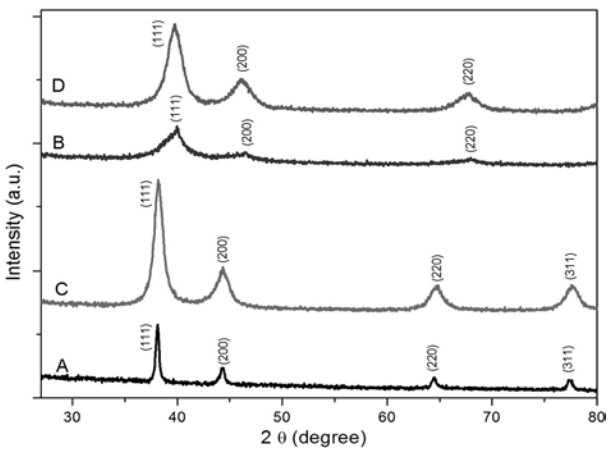

Fig. 4. XRD patterns of (A) MPTMS silica@Ag, (B) MPTMS silica@Au, (C) MPTMS silica@Pd, and (D) MPTMS silica@Pt.

To further determine whether noble matals have been coated on the surface of MPTMS silica particles and to get the information on the coordination state of the noble metals, XPS measurements were additionally performed. XPS has been proven to be a suitable technique for an investigation of the surface composition of core-shell nanoparticles. Fig. 5 shows the XPS spectra of the survey and each noble metal peak for silica@M (M = Ag, Au, Pd and Pt). The main peak of O 1 s generally located at around 533.5 eV is corresponding to the lattice oxygen of the SiO_2 matrices (Si-O-Si) [25]. In Fig. 5 of the survey spectra for silica@M, the O 1 s peak of MPTMS silica can be observed at around 532.2 eV. Although Si atoms of MPTMS silica are not substituted by transition metal atoms, the O 1 s peak shifts from 533.5 eV to a lower energy state of 532.2 eV. This phenomenon of the O 1 s peak shift has been explained by the typical structural property that Si atom of MPTMS silica was surrounded by three oxygen atoms in contrast to the general silica matrix (SiO_2). The initially performed XPS survey scan of the samples revealed the presence of C 1s, O 1s, S 2p, and noble matals shell levels of silica@M as shown in Fig. 5. Each noble metal peak for silica@M in the survey spectra clearly verified the existence of noble metals on the surface via each specific peak position and the quantity of coated noble metals on the surface via the intensity of these peaks. The bulk noble metals were observed with their typical binding energies (BE) representing Ag (BE = 368.3 eV), Au (BE = 84 eV), Pd (BE = 335.3 eV), and Pt (BE = 71.2 eV) [33-37]. Figs. 5(A), (B) show the XPS survey spectra of silica@Ag and silica@Pt particles. The binding energies of the Ag 3d and Pt 4f are similar to that of the respective bulk metals. However, the binding energies of Au 4f and Pd 3d were higher than that of the bulk metals. The positive shift in binding energy may be attributed to the partial oxidation and size effects of the crystalline nanoparticles created besides silica@M [35, 36]. In the Au (4f) region, the first component of the $4f_{7/2}$ peak located at ca. 84 eV, is generally assigned to photoelectrons originated from metallic Au $4f_{7/2}$ energy levels [33]. However, the inset of Fig. 5(B) shows that the doublet peaks of Au (4f) are located at 84.6 and 88.3 eV. The overall peak position is shifted to a higher binding energy by 0.6 eV. The higher binding energy of Au 4f peaks is likely to be indicative of the presence of both metallic Au (0) and Au (I) oxides because the Au $4f_{7/2}$ peak of oxidized Au was shown in a higher binding energy at 84.9 eV. In the Pd (3d) region, the first component of the Pd $3d_{5/2}$ peak was located at ca. 335.3 eV, which is close to photoelectrons originating from the metallic Pd $3d_{5/2}$ binding energy region. However, the inset of Fig. 5(C) shows that the doublet peaks of Pd (3d) are centered at 336.05 and 341.4 eV and that the overall peak position is also shifted to a higher BE by

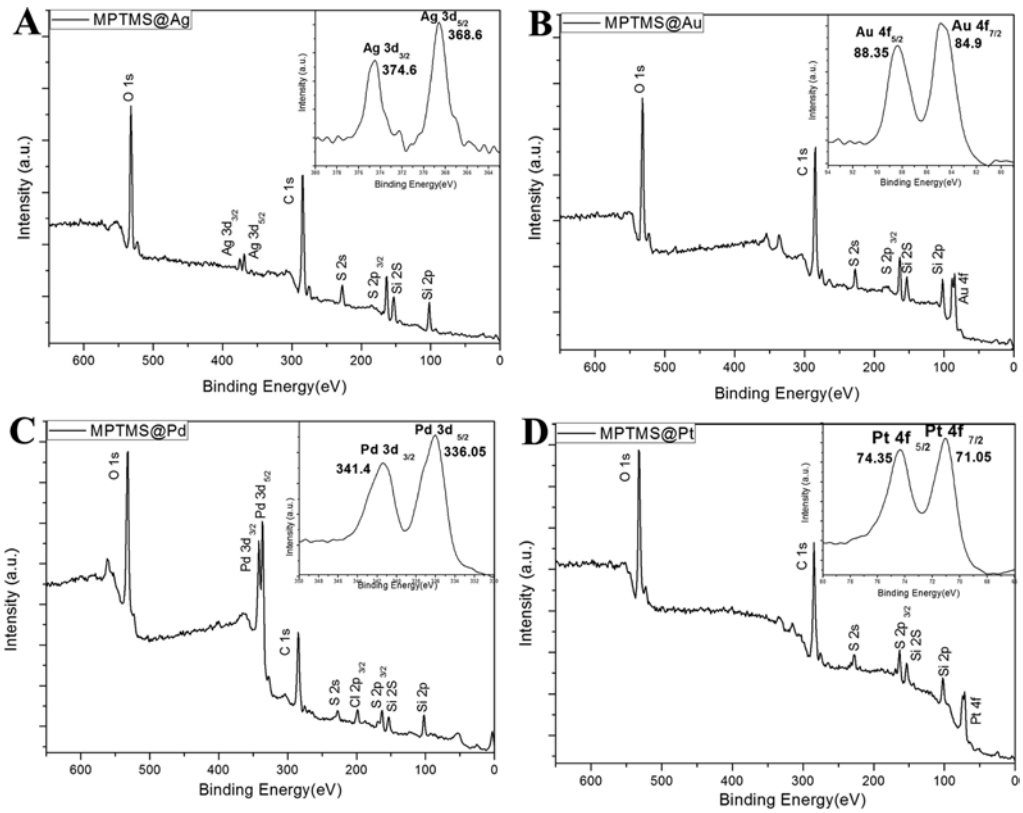

Fig. 5. XPS spectra of (A) MPTMS silica@Ag, (B) MPTMS silica@Au, (C) MPTMS silica@Pd, and (D) MPTMS silica@Pt (inset is XPS spectra of (A) Ag 3d, (B) Au 4f, (C) Pd 3d, and (D) Pt 4f).

0.75 eV and the Pd $3d_{5/2}$ peak showed a shoulder peak at the higher binding energy side of the main peak. The higher binding energy of Pd 3d peaks infers that Pd (0) and Pd (I) oxides coexisted in the sample because the Pd $3d_{5/2}$ peak of palladium oxides was observed with a higher binding energy at 336.5-338.0 eV [37]. Furthermore, the intensity of the Pd $3d_{5/2}$ peak in Fig. 5(C) is significantly higher than others because the many as-synthesized Pd nanoparticles besides the silica@Pd coexisted in the sample as shown in the SEM and XRD analysis. Therefore, silica@Pt indicated the purest metallic Pt shell with a high wall thickness in this study. Although the silica@Ag also indicated a high purity metallic Ag shell, the XRD widescan of Fig. 4(A) and XPS survey of Fig. 5(A) showed a low intensity and low level of crystallinity. Silica@Pt with a thick metallic Pt shell will enable application in various industrial fields. In this study, we tried to prepare hollow Pt metal spheres which be applied in diverse areas including photonics, photoelectronics, catalysis, etc.

Hollow Pt metal spheres were prepared by the removal of the silica template selectively using HF. When the Pt coated silica particles (Fig. 3(E)) were added to the HF solution, HF penetrated the core of the silica particles and only etches the silica material, and then the hollow metallic Pt spheres remain as a consequence. An SEM image of the Pt hollow particles in Fig. 6(A) shows that most of the particles have openings in the shell and a broken shape after mechanical fracture. This clearly supports the evidence of a hollow structure. Also, hollow spheres have a very narrow size distribution and the shell thickness is about 100 nm (inset of Fig. 6(A)), and the TEM image of Fig. 6(B) also reveals the hollow structure of the products more clearly. It can be seen that all of the spheres have a marked contrast with dark edges and bright centers, confirming a hollow structure. The inset of Fig. 6(B) shows a selected area electron diffraction (SAED) pattern of the sample. The presence of clear diffraction spots indicates that the hollow Pt spheres have a crystalline Pt structure from full growth and can be indexed to fcc (111), (200), (220), and (311) reflections.

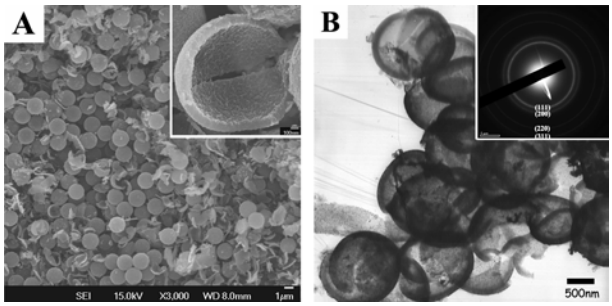

Fig. 6. (A) SEM and (B) TEM image of hollow Pt spheres (inset (A) is magnified image, and inset (B) is TEM selected area electron diffraction pattern of a hollow Pt sphere).

Conclusions

In summary, we have demonstrated that the synthesis of silica@M (M = Ag, Au, Pd, Pt) particles can be performed using highly monodispersed MPTMS silica as a substrate which was achieved via our previous studies. The use of highly monodispersed MPTMS silica as a substrate with a high coverage of thiol groups provides a successful pathway for the synthesis of noble metals coated silica and hollow metal spheres. This approach to synthesize silica@M is attractive for the following reasons; (1) a high loading capacity of noble metals due to the highly immobilized thiol groups on the surface of monodispersed MPTMS silica as a substrate, and a high yield of reproduction, (2) a high selectivity of the noble metal particles created from the reduction agent in the aqueous solution, (3) a high application for synthesis of various silica@M particles using other metal ions and diverse hollow metal particles, (4) the possibility of silica@M and hollow Pt particles for applications such as photonics, photoelectronics, catalysis, etc. The noble metal coated silica and hollow Pt metal spheres obtained here may be promising candidates for both fundamental research and applications. Thus, it can be expected that the strategy employed in this study can also be extended to the application for the synthesis of various metals coated silica and hollow metal spheres.

Acknowledgment

This work was supported by Basic Science Research Program through the National Research Foundation of Korea (NRF) grant funded from the Ministry of Education, Science and Technology (MEST) of Korea for the Center for Next Generation Dye-sensitized Solar Cells (No. 2010-0001842).

References

1. A. Khaleel, Colloid Surf. A 346 (2009) 130-137.
2. Q. Ge, X. Li, H. Kaneko and K. Fujimoto, J. Mol. Catal. A 278 (2007) 215-219.
3. S. Xu, B. Zhao, W. Xu and Y. Fan, Colloid Surf. A 257-258 (2005) 313-317.
4. P. Escribano, B. Julian-Lopez, J. Planelles-Arago, E. Cordoncillo, B. Viana and C. Sanchez, J. Mater. Chem. 18 (2008) 23-40.
5. P. Englebienne and A.V. Hoonacker, J. Colloid Interface Sci. 292 (2005) 445-454.
6. D. Wen, S.J. Guo, J.F. Zhai, L. Deng, W. Ren and S.J. Dong, J. Phys. Chem. C 113 (2009) 13023-13028.
7. S.J. Guo and S.J. Dong, Trac-Trends Anal. Chem. 28 (2009) 96-109.
8. W. Stöber, A. Fink and E. Bohn, J. Colloid Interface Sci. 26 (1968) 62-69.
9. H. Chen and J. He, J. Colloid Interface Sci. 316 (2007) 211-215.
10. T. Yokoi, Y. Sakamoto, O. Terasaki, Y. Kubota, T. Okubo and T. Tatsumi, J. Am. Chem. Soc. 128 (2006) 13664-13665.
11. F. Branda, B. Silvestri, G. Luciani and A. Costantini, Colloid Surf. A 299 (2007) 252-255.
12. J.M. Lee, Y.G. Lee, D.W. Kim, C. Oh, S.M. Koo and S.G. Oh, Colloid Surf. A 301 (2007) 48-54.
13. J.H. Park, Y.G. Kim, C. Oh, S.I. Shin, Y.C. Kim, S.G. Oh and S.H. Kong, Mater. Res. Bull. 40 (2005) 271-280.
14. J.H. Park, S.G. Oh and B.W. Jo, Mater. Chem. Phys. 87 (2004) 301-310.
15. T.H. Kim, D.W. Kim, J.M. Lee, Y.G. Lee and S.G. Oh, Mater. Res. Bull. 43 (2008) 1126-1134.
16. L.M. Bronstein, C.N. Linton, R. Karlinsey, E. Ashcraft, B.D. Stein, D.I. Svergun, M. Kozin, I.A. Khotina, R. J. Spontak, U. W. Zwanziger and J. W. Zwanziger, Langmuir 2003, 19, 7071-7083.
17. H. Pu, X. Zhang, J. Yuan and Z. Yang, J. Colloid Interface Sci. 331 (2009) 389-393.
18. I.P. Blitz, J.P. Blitz, V.M. Gun'ko and D.J. Sheeran, Colloid Surf. A 307 (2007) 83-92.
19. W. Wang and S.A. Asher, J. Am. Chem. Soc. 123 (2001) 12528-12535.
20. J. Liqiang, W. Baiqi, X. Baifu, L. Shudan, S. Keying, C. Weimin and F. Honggang, J. Solid State Chem. 177 (2004) 4221-4227.
21. D.W. Kim, J.M. Lee, J.J. Lee, P.Y. Kang, Y.C. Kim and S.G. Oh, Surf. Coat. Technol. 201 (2007) 7663-7667.
22. V. Iliev, D. tomova, L. Bilyarska, A. Eliyas and L. Petrov, Appl. Catal. B 63 (2006) 266-271.
23. C. Graf and A. V. Blaaderen, Langmuir 18 (2002) 524-534.
24. F. Caruso, Chem. Eur. J. 6 (2000) 413-419.
25. Y.G. Lee, J.H. Park, C. Oh, S.G Oh and Y.C. Kim, Langmuir 23 (2007) 10875-10878.
26. J.M. Lee, D.W. Kim, Y.D. Jun and S.G. Oh, Mater. Res. Bull. 41 (2006) 1407-1416.
27. B. Smith, Infrared spectral interpretation, a systematic approach, CRC Press, New York, USA, 1999.
28. A.O. Rami and E.R. Houssam, J. Mol. Struct. 919 (2009) 140-145.
29. A.S. Fernando, F. Sérgio, V.G. Marcus, R D. Marian and J.J. Miguel, J. Am. Ceram. Soc. 86 (2003) 1196-1201.
30. W. Xueguang, C. Soofin and C.C.C. Jerry, J. Phys. Chem. C 111 (2007) 2156-2164.
31. D. Isabel, M.A. Carlos, M. Federico, P.P. Joaquín and S. Enrique, J. Catalysis 193 (2000) 283-294.
32. L. Zhang, H.C.L. Abbenhuis, G. Gerritsen, N.N. Bhriain, P.C.M.M. Magusin, B. Mezari, W. Han, R.A. Santen, Q. Yang and C. Li, Chem. Eur. J. 13 (2007) 1210-1221.
33. C.D. Wanger, W.M. Riggs, L.E. Davis, J.F. Moulder and G.E. Muilenberg, Handbook of X-ray Photoelectron Spectroscopy Perkin-Elmer Corp., Eden Prairie, MN, 1978.
34. E.S. Martha, F.B. Helge and E.S. Mohammed, Adv. Funct. Mater. 18 (2008) 3179-3188.
35. Y.C. Liu and T.C. Chuang, J. Phys. Chem. B 107 (2003) 12383-12386.
36. C. Mangeney, S. Bousalem, C. Connan, M.J. Vaulay, S. Bernard and M.M. Chehimi, Langmuir 22 (2006) 10163-10169.
37. J. Xiao, Y. Xie, R. Tang, M. Chen and X. Tian, Adv. Mater. 13 (2001) 1887-1891.